

# Frequency-Agile Bandstop Filter with Tunable Attenuation

Douglas R. Jachowski and Christen Rauscher

Microwave Technology Branch, Electronics Science and Technology Division  
Naval Research Laboratory, Washington, DC 20375 USA

**Abstract** — A frequency-agile bandstop filter technology with tunable stopband attenuation and constant absolute bandwidth is described. The technology is demonstrated by a six-resonator planar microstrip filter with simultaneous varactor-diode tuning of stopband attenuation from 30dB to 50dB and of operating frequency from 1.8 GHz to 2.2 GHz, with a stopband bandwidth of 60 MHz and absolute 3dB bandwidth of less than 390 MHz.

## I. INTRODUCTION

Receiver applications sometimes call for discerning weak signals in the presence of much stronger signals. Unfortunately, the stronger signals can drive the receiver front-end amplifier into compression or saturation – distorting, compressing, and masking weaker signals, desensing the receiver. Recently, compact narrowband absorptive bandstop, or “notch”, filters have been demonstrated that can selectively eliminate fixed-frequency or frequency-hopping interferers using lossy circuit components [1]-[6]. However, there are occasions when it is desirable to receive both weak and strong signals, attenuating the strong signals only just enough to keep the amplifier operating linearly. This paper addresses such a need by describing an extension of the circuit in [2] that enables tuning of the stopband attenuation level of a frequency-agile absorptive notch filter without the need for additional components. Although it is conventionally possible to tune attenuation by tuning bandwidth, the new approach allows tuning of stopband attenuation while preserving both stopband and passband bandwidths. This new circuit component could also be called a “frequency-agile frequency-selective variable attenuator.”

Due to their relative simplicity, “first-order” absorptive filters tend to be the most practical to use in frequency-agile applications, but attenuation characteristics of such first-order sections alone tend to lack sufficient stopband bandwidth to be of practical use. Consequently, first-order sections are cascaded to realize practical stopband bandwidths [2], [7]. This paper investigates such a “third-order”, six-resonator, microstrip absorptive bandstop filter – composed of a properly phased cascade of three “first-order” stages – with a 22% frequency tuning range and a 20dB stopband-attenuation tuning range. Unlike the filters of [8], attenuation is tuned by tuning varactor capacitance (i.e., resonator frequencies) rather than FET resistance.

## II. THE TUNABLE “ABSORPTIVE-PAIR” NOTCH FILTER

Conventional bandstop filters reflect stopband signals, and resonator loss tends to reduce and limit their stopband attenuation and band-edge selectivity. In [2], a two-resonator bandstop filter topology, termed an “absorptive-pair”, was introduced that, to at least some extent, absorbs stopband signals – with resonator loss limiting minimum bandwidth rather than stopband attenuation. One of many possible electrically-equivalent circuit schematics of an absorptive pair is given in Fig. 1, in which ideal (frequency invariant) admittance inverters  $k_{01}$  couple lossy lumped-element resonators, with admittances  $Y_p$  and  $Y_m$ , to the ends of a phase shift element of characteristic admittance  $Y_s$  and frequency-invariant phase shift  $\phi$ , while ideal admittance inverter  $k_{11}$  directly couples the two resonators. Although a more accurate analysis would require frequency dependent representations of couplings and phase shifts, including frequency dependence would lead to more complicated results which obscure understanding. Fig. 2 shows representative transmission responses of the highpass prototype of the filter of Fig. 1.

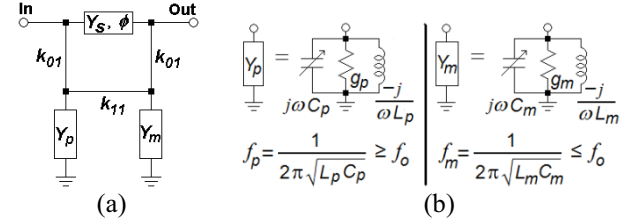


Fig. 1. Equivalent circuit of a “first-order”, two-resonator, absorptive bandstop filter with tunable stopband attenuation.

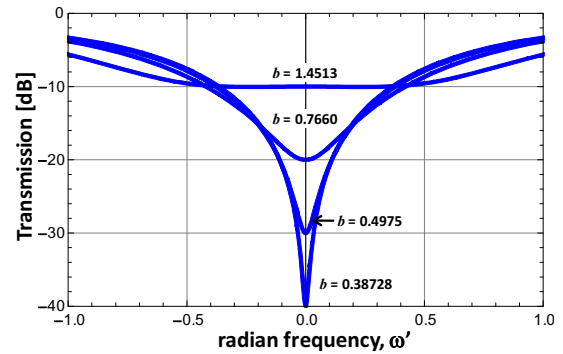


Fig. 2. Simulated responses of an absorptive-pair highpass prototype filter illustrating tunable attenuation levels of 10, 20, 30, and 40 dB at  $\omega'=0$ , assuming  $Y_s=1$ ,  $k_{11}=g=1$ ,  $q_u=2$ , and (from (10))  $k_{01}=\sqrt{Y(k_{11}^2+g^2+b_o^2)/(k_{11}\sin)}$  with  $b_o=0.326$ .

### A. Analysis of the Absorptive Pair

For the idealized absorptive-pair notch filter in Fig. 1:

$$Y_p = g_p (1 + jQ_p \alpha_p) \quad (1)$$

$$Y_m = g_m (1 + jQ_m \alpha_m) \quad (2)$$

where

$$\begin{aligned} Q_p &= 2\pi f_p C_p / g_p, \quad Q_m = 2\pi f_m C_m / g_m, \\ \alpha_p &= (f / f_p - f_p / f), \quad \alpha_m = (f / f_m - f_m / f), \\ f_p &= 1 / (2\pi \sqrt{L_p C_p}), \text{ and } f_m = 1 / (2\pi \sqrt{L_m C_m}). \end{aligned}$$

Although the phase shift element could be implemented in many ways, such as by a parallel-coupled-line phase shifter or lowpass or highpass filter, here a transmission line of admittance  $Y_s$  and electrical length  $\phi$  at filter center frequency  $f_o$  is used. The reciprocal asymmetric network in Fig. 1 may be analyzed using ABCD parameter analysis [9, pp. 7-14, 68-73]. Assuming equal source and load impedances,  $R_s = R_L = Z_s = 1/Y_s$ , the two-port scattering parameter  $S_{21}$  is given by [9, p. 52]

$$S_{21} = \frac{2Z_s}{B + (A + D)Z_s + CZ_s^2} \quad (3)$$

where

$$A = (Y_s(k_{11}^2 + Y_p Y_m) \cos(\phi) + jk_{01}^2 Y_p \sin(\phi)) / d \quad (4)$$

$$D = (Y_s(k_{11}^2 + Y_p Y_m) \cos(\phi) + jk_{01}^2 Y_m \sin(\phi)) / d$$

$$B = j((k_{11}^2 + Y_p Y_m) \sin(\phi)) / d$$

$$C = (k_{01}^2 Y_s (Y_p + Y_m) \cos(\phi) + j((k_{01}^4 + Y_s^2(k_{11}^2 + Y_p Y_m)) \sin(\phi) - 2k_{01}^2 k_{11} Y_s)) / d$$

$$d = Y_s(k_{11}^2 + Y_p Y_m) - k_{01}^2 k_{11} \sin(\phi).$$

To better understand the behavior of the absorptive bandstop filter it is most convenient to work with its highpass prototype, with a minimum of attenuation  $L_o$  at radian frequency  $\omega = 0$ . The highpass prototype can be represented by Fig. 1(a), with  $Y_p$  and  $Y_m$  replaced by

$$Y_p' = g(1 + j(\omega' q_u + b/g)) \text{ and} \quad (5)$$

$$Y_m' = g(1 + j(\omega' q_u - b/g)) \quad (6)$$

as shown in Fig. 3, where  $b$  is a variable frequency-invariant susceptance,  $g$  is a conductance,  $\omega'$  is the normalized highpass prototype radian frequency,  $q_u = \omega' c / g$  is the unloaded Q of the shunt admittances of the highpass prototype,  $c$  is a capacitance, and  $\omega'_1 = 1$  is the band-edge radian frequency at which the attenuation is  $L_s$ .

In terms of  $s' = j\omega'$ ,  $S_{21}$  is given by

$$S_{21}(j\omega') = e^{-j\phi} \frac{(s' - s'_{z1})(s' - s'_{z2})}{(s' - s'_{p1})(s' - s'_{p2})} \quad (7)$$

with zeros at

$$s'_{z1,2} = -\left(\frac{1}{q_u}\right) \left(1 \pm \frac{1}{g Y_s} \sqrt{Y_s k_{01}^2 k_{11} \sin[\phi] - Y_s^2 (k_{11}^2 + b^2)}\right) \quad (8)$$

and poles at

$$s'_{p1,p2} = \frac{-(k_{01}^2 + 2gY_s \pm e^{-j\phi} \sqrt{(k_{01}^2 + j2k_{11}Y_s e^{j\phi})^2 - (2bY_s e^{j\phi})^2})}{2gY_s q_u}. \quad (9)$$

Using (3) – (10), equating the numerator of  $S_{21}$  to zero at  $\omega' = 0$ , and solving provides the design criteria that gives the absorptive highpass prototype filter of Figs. 1(a) and 3 infinite attenuation at  $\omega' = 0$  [2]:

$$k_{01} = \sqrt{Y_s \frac{k_{11}^2 + g^2 + b^2}{k_{11} \sin(\phi)}} \quad (10)$$

A similar analysis of the bandstop filter of Fig. 1 using (1) – (4) and  $S_{21}|_{f=f_o} = 0$  gives a design criteria of

$$k_{01} = \sqrt{Y_s \frac{k_{11}^2 + g_m g_p + g_m g_p Q_m Q_p (f_p^2 - f_o^2)(f_o^2 - f_m^2) / f_o^2}{k_{11} \sin(\phi)}} \quad (11)$$

where the frequency of infinite stopband attenuation is

$$f_o = \sqrt{f_m f_p \frac{Q_m f_m + Q_p f_p}{Q_m f_p + Q_p f_m}}. \quad (12)$$

Assuming  $g \approx g_m \approx g_p$  and  $Q_o \approx Q_m \approx Q_p$ , (12) becomes

$$f_o \approx \sqrt{f_m f_p}, \quad (13)$$

and from (10) and (11) the resonant frequencies are

$$f_p, f_m \approx f_o \left( \sqrt{1 + \left(\frac{b}{2gQ_o}\right)^2} \pm \frac{b}{2gQ_o} \right) \quad (14)$$

and the prototype's frequency-invariant susceptance  $b$  is proportional to the difference in resonant frequencies  $f_p, f_m$  of the two resonators in the corresponding bandstop filter:

$$b \approx (f_p - f_m) \frac{gQ}{f_o} \quad (15)$$

Using (8) and (9), and letting  $k_{01}$  in (10) be a constant with  $b = b_o = 0.326$ , Figs. 2 and 4 illustrate the dependence of the highpass prototype's stopband attenuation level on  $b$ , and, by analogy, the dependence of the corresponding bandstop filter's stopband level on  $(f_p - f_m)$ .

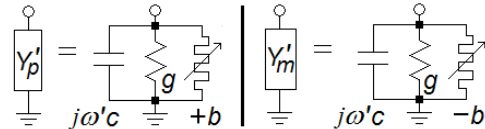


Fig. 3. Definitions for admittances  $Y_p'$  and  $Y_m'$ , which replace  $Y_p$  and  $Y_m$  in Fig. 1 to form the first-order highpass prototype.

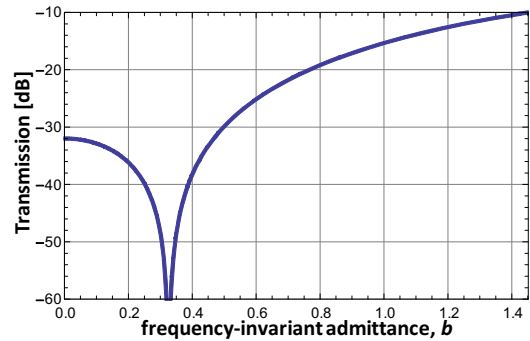


Fig. 4. Plot of transmission versus  $b$  for the absorptive-pair highpass prototype at  $\omega'=0$ , assuming  $Y_s=1$ ,  $k_{11}=g=1$ ,  $q_u=2$ , and (from (10))  $k_{01} = \sqrt{Y(k_{11}^2 + g^2 + b_o^2) / (k_{11} \sin)}$  with  $b_o=0.326$ .

### B. Frequency-Agile Absorptive-Pair Bandstop Filter

To demonstrate the capabilities of the absorptive-pair, an improved implementation of the frequency-agile bandstop filter demonstrated in [2] was designed using an iterative-analysis, manual-optimization approach, resulting in the layout of Fig. 5(a) and the manufactured unit of Fig. 5(b). The design process began by (a) characterizing the microstrip loss on the Rogers' RO4003 substrate (60-mil thick, 3.38 dielectric constant, 0.0021 dielectric loss tangent, 0.034 mm copper) by matching measurements of a conventional notch filter (with a single, open-circuited, half-wavelength resonator) to corresponding microstrip models in commercially-available circuit and 3D planar electromagnetic (EM) field simulators (by adjusting conductor resistivity) and (b) extracting the series-resistor-inductor-capacitor (series-RLC) model of the varactors, in Fig. 6, from two-port s-parameter measurements of a 50Ω microstrip line with a shunt-connected reverse-biased varactor diode to ground. Then a microstrip circuit model, topologically representative of Fig. 1, was iteratively-optimized at three operating frequencies: a lowest tuned frequency of about 1.5GHz, a highest tuned frequency of about 2.5GHz, and a mid-band tuned frequency of 2GHz. Experience with [2] indicated that the design should constrain the resonant frequencies of the resonators to be equal at the target lowest-tuned frequency and constrain one of the two bias voltages to be the highest acceptable voltage at the target highest-tuned frequency.

Once the circuit model's attenuation was greater than 60dB at each of the three operating frequencies for some set of bias voltage pairs, ad-hoc lowpass varactor bias networks, comprised of three sections of meandered (electrically quarter-wavelength) microstrip were added, with intervening 20pF shunt capacitors to ground. After the circuit had been re-optimized, subcircuits were gradually replaced by s-parameter files of corresponding EM-modeled microstrip layouts, and further re-optimized, until the entire circuit model (except varactors and capacitors) had been replaced by a collection of s-parameter files corresponding to different portions of EM-modeled microstrip layouts (dielectric overlay sections, center section, bias lines, and varactor grounding vias).

It was beneficial to keep the varactor ground vias as far apart as practical to minimize their coupling, to design the isolation level of the bias networks to be similar to the maximum attenuation of the filter (about 60dB), and to mount the bypass capacitors vertically as substrate feedthroughs to minimize their inductance to ground and keep the associated series resonances above the frequency band of interest. Simulations and measurements of the filter's performance are compared in Fig. 7(a) and a plot of measured maximum-attenuation frequency versus the difference between the two bias voltages is given in Fig. 7(b) – corroborating the theory in section II(a).

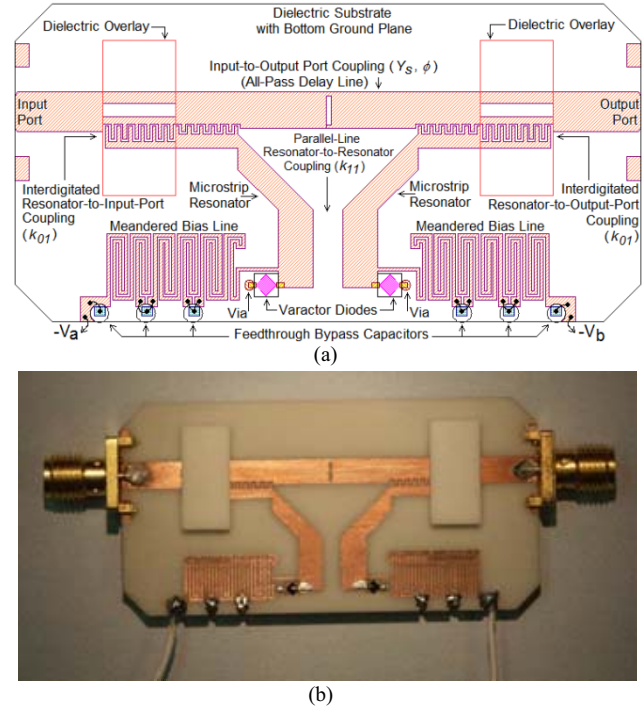


Fig. 5. Annotated layout (a) and photo (b) of the frequency-agile first-order, absorptive-pair filter with tunable attenuation. Dielectric overlays are used to increase certain couplings [10].

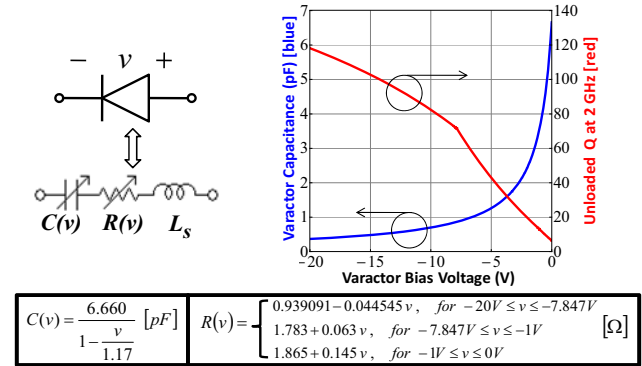


Fig. 6. Model of the reverse-biased Metelics MGV-125-24-E25 GaAs hyperabrupt varactor diode, with  $L_s = 1.327$  nH.

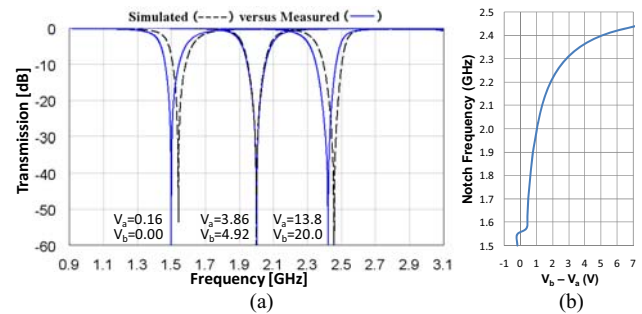


Fig. 7. (a) Superimposed plots of the predicted and measured transmission of the filter of Fig. 5 tuned to 3 different frequencies. (b) Measured notch frequency versus difference in the reverse-bias voltages applied to the two varactors.

### III. THE TUNABLE THIRD-ORDER BANDSTOP FILTER

Three of the frequency-agile, first-order, absorptive-pair bandstop filter stages of the preceding section were connected in cascade by two  $52.7\Omega$  microstrip lines, each approximately  $30^\circ$  long at 2GHz, resulting in the integrated third-order, six-resonator bandstop filter shown in Fig. 8. Superimposed plots of the measured characteristics of the filter are shown in Fig. 9, where the filter has been tuned to attenuation levels of 30, 35, 40, 45, and 50 dB at operating frequencies of 1.8, 2.0, and 2.2 GHz by bias voltages shown in Fig. 10. Stopband bandwidths are all tuned to 60 MHz and the resulting absolute 3dB bandwidths are all less than 390 MHz.

### IV. CONCLUSION

A first-order (two-resonator) absorptive bandstop filter with tunable stopband attenuation has been introduced along with a theory of its design and operation. The circuit concept does not rely on particular tuning components or manufacturing technologies. A cascade of three first-order sub-circuits is used to make a third-order filter. Unlike the filters of [8], it exhibits useful levels of frequency selectivity, passband insertion loss, and stopband bandwidth, and demonstrates simultaneous and substantial tunability of operating frequency and stopband attenuation while maintaining constant stopband and 3dB bandwidths. Filters of this type may be useful in receivers that must simultaneously handle widely different signal levels.

### ACKNOWLEDGEMENT

Thanks to Dave Brown of Brown-Wolf Engineering for suggesting this effort, Frank Patten of DARPA for supporting this effort, and Rogers Corp. for the substrate.

### REFERENCES

- [1] D. R. Jachowski, "Passive enhancement of resonator Q in microwave notch filters," *IEEE MTT-S Int. Microw. Symp. Dig.*, pp. 1315-1318, June 2004.
- [2] D. R. Jachowski, "Compact, frequency-agile, absorptive bandstop filters," *IEEE MTT-S Int. Microw. Symp. Dig.*, June 2005.
- [3] A. C. Guyette, I. C. Hunter, R. D. Pollard, and D. R. Jachowski, "Perfectly-matched bandstop filters using lossy resonators," *IEEE MTT-S Int. Microw. Symp. Dig.*, June 2005.
- [4] D. R. Jachowski, "Cascadable lossy passive biquad bandstop filter," *IEEE MTT-S Int. Microw. Symp. Dig.*, pp. 1213-1216, June 2006.
- [5] D. R. Jachowski, "Synthesis of lossy reflection-mode bandstop filters," in *Proc. Int. Workshop on Microwave Filters*, CNES, Toulouse, France, 16-18 October 2006.
- [6] P. W. Wong, I. C. Hunter, and R. D. Pollard, "Matched Bandstop Resonator with Tunable K-Inverter," *Proc. 37<sup>th</sup> Eur. Microw. Conf.*, pp. 664-667, Oct. 2007.
- [7] I. Hunter, A. Guyette, R. D. Pollard, "Passive microwave receive filter networks using low-Q resonators," *IEEE Microw. Mag.*, pp. 46-53, Sept. 2005.
- [8] S. Toyoda, "Notch filters with variable center frequency and attenuation," *IEEE MTT-S Int. Microw. Symp. Dig.*, pp. 595-598, June 1989.
- [9] J. A. Dobrowolski, *Introduction to Computer Methods for Microwave Analysis and Design*, (Artech: 1991).
- [10] B. Sheleg and B. E. Spielman, "Broadband directional couplers using microstrip with dielectric overlays," *IEEE Trans. Microw. Theory Tech.*, pp. 1216-1220, Dec. 1974.



Fig. 8. Photograph of the frequency-agile, third-order absorptive-pair bandstop filter with tunable attenuation.

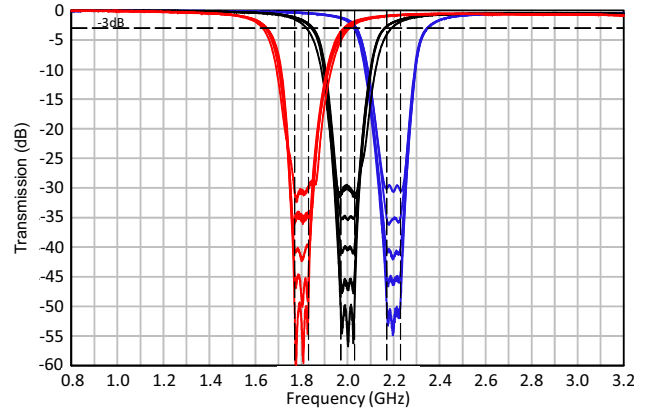


Fig. 9. Superimposed plots of the measured transmission of the bandstop filter of Fig. 8 demonstrating both tunable operating frequency and tunable stopband attenuation.

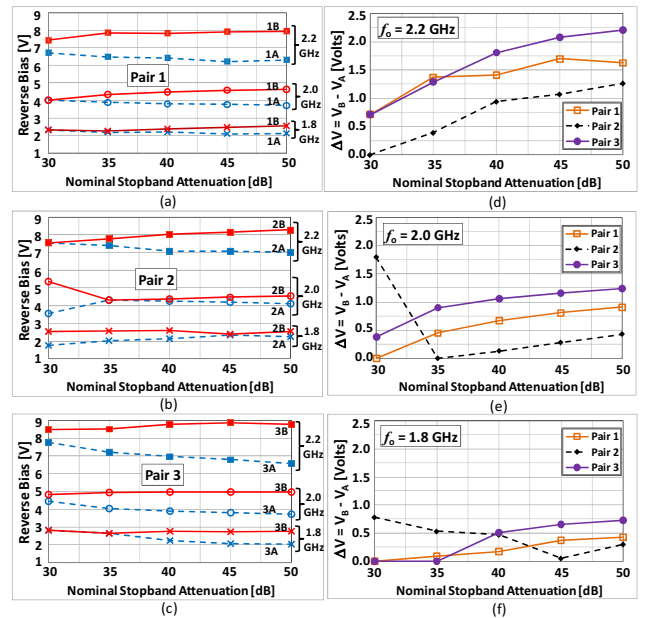


Fig. 10. Plots of stopband attenuation and operating frequency as a function of bias voltages for the varactors of the filter's (a) first, (b) second, and (c) third absorptive-pair stage, as well as plots relating difference in bias voltages for specified pairs of varactors to stopband attenuation at operating frequencies of (d) 2.2 GHz, (e) 2.0 GHz, and (f) 1.8 GHz.